

# Effect of Metal Ion and Water Coordination on the Structure of a Gas-Phase Amino Acid

Rebecca A. Jockusch, Andrew S. Lemoff, and Evan R. Williams\*

Contribution from the Department of Chemistry, University of California, Berkeley, California 94720-1460

Received March 14, 2001

**Abstract:** The mode of metal ion and water binding to the amino acid valine is investigated using both theory and experiment. Computations indicate that without water, the structure of valine is nonzwitterionic. Both  $\text{Li}^+$  and  $\text{Na}^+$  are coordinated to the nitrogen and carbonyl oxygen (NO coordination), whereas  $\text{K}^+$  coordinates to both oxygens (OO coordination) of nonzwitterionic valine. The addition of a single water molecule does not significantly affect the relative energies calculated for the cationized valine clusters. Experimentally, the rates of water evaporation from clusters of  $\text{Val}\cdot\text{M}^+(\text{H}_2\text{O})_1$ ,  $\text{M} = \text{Li}, \text{Na}, \text{and K}$ , are measured using blackbody infrared radiative dissociation. The dissociation rate from the valine complex is compared to water evaporation rates from model complexes of known structure. These results indicate that the metal ion in the lithiated and the sodiated clusters is NO-coordinated to nonzwitterionic valine, while that in the potassiated cluster has OO coordination, in full agreement with theory. The zwitterionic vs nonzwitterionic character of valine in the potassiated cluster cannot be distinguished experimentally. Extensive modeling provides strong support for the validity of inferring structural information from the kinetic data.

## Introduction

Biological processes, including signal transduction, control of reaction specificity, and macromolecular structure, depend on electrostatic interactions among the polar and ionic species ubiquitous in living systems.<sup>1</sup> Proteins and nucleic acids contain numerous charged functionalities. Free metal ions provide electrochemical gradients necessary for cellular function, and they also serve as messengers. Binding of metal ions is crucial to the function of many enzymes. A dramatic example is the sequence of events which is triggered by a small flux of calcium ions;  $\text{Ca}^{2+}$  coordinates to multiple oxygens in proteins, such as calmodulin, which then undergo a large structural change, become activated, and in turn activate other proteins including those involved in muscle contraction.<sup>2</sup>

The intrinsic stability of biomolecules with charged functionalities is determined by the gas-phase acidities and basicities of these groups. Ionic species are further stabilized in several ways. Counterions provide favorable electrostatic interactions. Solvation of charges by polar species, especially water, also provides significant stabilization. Increased knowledge of these interactions is vital to the understanding and prediction of biomolecular properties in vivo. Gas-phase studies of simplified systems, such as single amino acids, metal ions, and/or individual water molecules, provide a means for investigating these effects individually.

While amino acids in solution exist as zwitterions over a wide range of pH, the most stable form of isolated amino acids in the gas phase is nonzwitterionic. For glycine (Gly), the nonzwitterionic form is calculated to be 19.3 kcal/mol more stable than the zwitterionic form.<sup>3</sup> Calculations show no barrier

to proton transfer and thus predict that the Gly zwitterion is not even a stable species in the gas phase in the absence of other stabilizing forces. To the best of our knowledge, no experimental evidence for the gas-phase Gly zwitterion or any other ground-state amino acid zwitterion has been reported.<sup>4–8</sup>

The zwitterionic form of amino acids can be stabilized by the presence of counterions, resulting in stable salt-bridge structures. Calculations on Gly·alkali metal cation ( $\text{M}^+$ ) complexes predict significant stabilization of salt-bridge structures. However, structures in which the Gly is nonzwitterionic (charge-solvated structures) are found to be 1–3 kcal/mol more stable than the salt-bridge forms.<sup>9–11</sup> According to these studies, the mode of metal ion complexation in the charge-solvated structures changes with the size of  $\text{M}^+$ . Small metal ions ( $\text{Li}^+$  and  $\text{Na}^+$ ) interact with both the nitrogen and carbonyl oxygen (NO coordination) in the lowest-energy conformers, while larger metal ions interact with both oxygens of the carboxylic group (OO coordination).

The strength of the electrostatic interaction is extremely important in the stabilization of salt bridges. For example, while Gly· $\text{Cu}^+$  adopts a charge-solvated structure in which the metal ion is NO-coordinated, Gly· $\text{Cu}^{2+}$  forms an OO-coordinated salt bridge.<sup>12</sup> Computational studies of Gly· $\text{M}^{2+}$ ,  $\text{M} = \text{Be}, \text{Mg}, \text{Ca}, \text{Sr}, \text{and Ba}$  illustrate the combined effects of metal ion size and

(1) Stryer, L. *Biochemistry*, 3rd ed.; W. H. Freeman, & Co.: New York, 1988.

(2) Creighton, T. E. *Proteins: Structures and Molecular Properties*, 2nd ed.; W. H. Freeman & Co.: New York, 1993.

(3) Yu, D.; Armstrong, D. A.; Rauk, A. *Can. J. Chem.* **1992**, *70*, 1762–1772.

(4) Suenram, R. D.; Lovas, F. J. *J. Mol. Spectrosc.* **1978**, *72*, 372–382.

(5) Locke, M. J.; McIver, R. T., Jr. *J. Am. Chem. Soc.* **1983**, *105*, 4226–4232.

(6) Iijima, K.; Tanaka, K.; Onuma, S. *J. Mol. Struct.* **1991**, *246*, 257–266.

(7) Godfrey, P. D.; Brown, R. D. *J. Am. Chem. Soc.* **1995**, *117*, 2019–2023.

(8) Chapo, C. J.; Paul, J. B.; Provencal, R. A.; Roth, K.; Saykally, R. J. *J. Am. Chem. Soc.* **1998**, *120*, 12956–12957.

(9) Jensen, F. *J. Am. Chem. Soc.* **1992**, *114*, 9533–9537.

(10) Hoyau, S.; Ohanessian, G. *Chem. Eur. J.* **1998**, *4*, 1561–1569.

(11) Wyttenbach, T.; Bushnell, J. E.; Bowers, M. T. *J. Am. Chem. Soc.* **1998**, *120*, 5098–5103.

(12) Bertran, J.; Rodriguez-Santiago, L.; Sodupe, M. *J. Phys. Chem. B* **1999**, *103*, 2310–2317.

charge.<sup>13</sup> The most stable charge-solvated form of Gly·Be<sup>2+</sup> is lower in energy than the salt bridge by 5–8 kcal/mol. However, the salt-bridge form is dramatically stabilized for complexes with the larger divalent cations and is 5–12 kcal/mol lower in energy than the charge-solvated structures.

Zwitterions and salt bridges can also be stabilized by increasing the acidity and basicity of the proton donating and accepting groups, respectively. For example, the guanidino group of the arginine (Arg) side chain is significantly more basic than an amino acid's N-terminus. Unlike Gly, the nonzwitterionic and zwitterionic forms of Arg are much closer in energy.<sup>14,15</sup> High-level calculations find that the nonzwitterionic form of Arg is more stable by <1 kcal/mol.<sup>15</sup> Cavity ring down experiments reveal the presence of only the nonzwitterionic isomer.<sup>8</sup>

In the presence of a charged metal ion, the structure of Arg is a delicate balance between a charge-solvated structure in which Arg folds around and solvates the metal ion and a salt bridge in which Arg is a zwitterion. An experimental and theoretical investigation of the structure of Arg–alkali metal cation complexes reveals an increase in stability of the salt-bridge relative to charge-solvated forms as the size of the cation increases. For M = K, Rb, and Cs, the salt-bridge form is calculated to be more stable than the charge-solvated form by ~3 kcal/mol.<sup>16</sup>

Bowers and co-workers have recently reported a correlation between proton affinities (PA) and structures of Gly·M<sup>+</sup> and glycine analogue·M<sup>+</sup> complexes for M = Na and Rb.<sup>17</sup> They have used this simple correlation to predict the most stable form of many cationized amino acids. Ion mobility experiments were done to try to verify these predictions, but calculated collision cross-sections for charge-solvated and salt-bridge conformations of the Gly·M<sup>+</sup> complexes are too similar to be able to distinguish in the experiment. Very recently, Bertran and co-workers have shown that substituting hydrogen atoms for chlorine atoms on the amino group of Gly decreases the basicity of the nitrogen, and thus destabilizes the Gly analog·M<sup>+</sup> salt-bridge structures.<sup>18</sup>

Gas-phase zwitterions and salt bridges can also be stabilized by solvating the charges. This solvation can be intramolecular, as is the case with bradykinin, a nine-residue peptide that, when singly protonated, exists in the gas phase as a salt bridge.<sup>19–22</sup> The positively charged Arg groups on either end of this molecule appear to be stabilized by interactions with the carbonyl oxygens of the peptide backbone. Focusing on just the amino acids forming the salt bridge in this peptide, the structure of the proton-bound dimer of Arg has also been investigated. Experiments show that this dimer is also bound together as a salt bridge

in which one of the Arg is a zwitterion, indicating that the solvation provided by the protonated Arg alone is enough to stabilize the zwitterionic Arg.<sup>14</sup>

Charges can also be stabilized through interactions with multiple polar solvent molecules such as water. Klassen and co-workers have reported sequential free energies of hydration to two different protonated amino acids and used these measurements to infer that the unhydrated protonated Gly does not undergo proton-induced cyclization, while protonated lysine is cyclized in the gas phase.<sup>23</sup> To the best of our knowledge, the only studies investigating the structures of gas-phase amino acid–water complexes reported to date are theoretical although there are several experimental studies of hydrated amino acid analogues.<sup>24–28</sup> Calculations indicate that two water molecules can make the zwitterionic form of Gly a local minimum on the potential energy surface.<sup>29</sup> However, the nonzwitterion is favored by 4–12 kcal/mol.<sup>30</sup> With the addition of a third water molecule, the zwitterionic Gly and nonzwitterionic Gly have comparable stability.<sup>31</sup>

Here, we use both theory and experiment to investigate structures of Val·M<sup>+</sup> and Val·M<sup>+</sup>(H<sub>2</sub>O), M = Li, Na, and K. This system was chosen as a simple model with which to begin a systematic study of specific interactions present between metal ions and the building blocks of proteins in an aqueous environment. We examine trends in the conformation as a function of both metal ion size and attachment of one water molecule. This study is the first step toward investigation of the gas-phase solvation of these complexes and determination of the number of water molecules required to convert a cationized amino acid from the most favorable gas-phase structure to the preferred structure in bulk solution.

## Experimental Section

**Chemicals.** Valine (Val) was purchased from Sigma Chemical Co. (Saint Louis, MO). Betaine (Bet) and alanine ethyl ester (AlaOEt) hydrochloride were purchased from Aldrich Chemical Co. (Milwaukee, WI). The structures of the amino acid and amino acid analogues (AA = Val, Bet, and AlaOEt) used are shown in Scheme 1. Hydroxides and chloride salts of Li, Na, and K were obtained from Fisher Scientific (Fair Lawn, NJ). All chemicals were used as purchased. Solutions for electrospray were made to mM AA, 1 mM metal (M) with deionized water. Chloride salts were used for Val·M<sup>+</sup> and Bet·M<sup>+</sup> solutions. Hydroxides were found to give much better signal for AlaOEt·M<sup>+</sup> (which came as an HCl salt) and were used to form cation adducts with this isomer. Control experiments in which AlaOEt·M<sup>+</sup> clusters were made with the chloride salts and experiments in which Val·M<sup>+</sup> and Bet·M<sup>+</sup> clusters were made with metal hydroxides were also performed to ensure that the difference in solution preparation did not effect the measured kinetics.

**Mass Spectrometry.** All dissociation experiments were performed on a home-built Fourier transform mass spectrometer with a 2.7 T

(13) Strittmatter, E. F.; Lemoff, A. S.; Williams, E. R. *J. Phys. Chem. A* **2000**, *104*, 9793–9796.

(14) Price, W. D.; Jockusch, R. A.; Williams, E. R. *J. Am. Chem. Soc.* **1997**, *119*, 11988–11989.

(15) Maksic, Z. B.; Kovacevic, B. *J. Chem. Soc., Perkin Trans. 2* **1999**, 2623–2629.

(16) Jockusch, R. A.; Price, W. D.; Williams, E. R. *J. Phys. Chem. A* **1999**, *103*, 9266–9274.

(17) Wytenbach, T.; Witt, M.; Bowers, M. T. *J. Am. Chem. Soc.* **2000**, *122*, 3458–3464.

(18) Pulkkinen, S.; Noguera, M.; Rodriguez-Santiago, L.; Sodupe, M.; Bertran, J. *Chem. Eur. J.* **2000**, *6*, 4393–4399.

(19) Schnier, P. D.; Price, W. D.; Jockusch, R. A.; Williams, E. R. *J. Am. Chem. Soc.* **1996**, *118*, 7178–7189.

(20) Deery, M. J.; Summerfield, S. G.; Buzy, A.; Jennings, K. R. *J. Am. Soc. Mass Spectrom.* **1997**, *8*, 253–261.

(21) Gimon-Kinsel, R. E.; Barbacci, D. C.; Russell, D. H. *J. Mass Spectrom.* **1999**, *34*, 124–136.

(22) Strittmatter, E. F.; Williams, E. R. *J. Phys. Chem. A* **2000**, *104*, 6069–6076.

(23) Klassen, J. S.; Blades, A. T.; Kebarle, P. J. *Phys. Chem.* **1995**, *99*, 15509–15517.

(24) Robertson, E. G.; Hockridge, M. R.; Jelfs, P. D.; Simons, J. P. *Phys. Chem. Phys.* **2001**, *3*, 786–795.

(25) Robertson, E. G.; Hockridge, M. R.; Jelfs, P. D.; Simons, J. P. *J. Phys. Chem. A* **2000**, *104*, 11714–11724.

(26) Mons, M.; Dimicoli, I.; Tardivel, B.; Piuze, F.; Robertson, E. G.; Simons, J. P. *J. Phys. Chem. A* **2001**, *105*, 969–973.

(27) Carles, S.; Lecomte, F.; Schermann, J. P.; Desfrancois, C. *J. Phys. Chem. A* **2000**, *104*, 10662–10668.

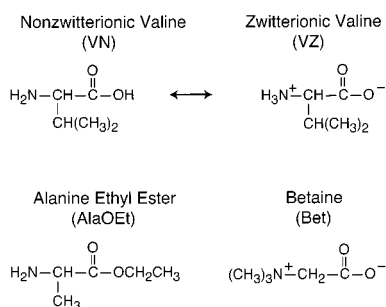
(28) Carles, S.; Desfrancois, C.; Schermann, J. P.; Smith, D. M. A.; Adamowicz, L. *J. Chem. Phys.* **2000**, *112*, 3726–3734.

(29) Jensen, J. H.; Gordon, M. S. *J. Am. Chem. Soc.* **1995**, *117*, 8159–8170.

(30) Tajkhorshid, E.; Jalkanen, K. J.; Suhai, S. *J. Phys. Chem. B* **1998**, *102*, 5899–5913.

(31) Kassab, E.; Langlet, J.; Evleth, E.; Akacem, Y. *J. Mol. Struct. (THEOCHEM)* **2000**, *531*, 267–282.

## Scheme 1



superconducting magnet. This instrument has been described previously.<sup>32</sup> We have recently installed a new temperature-controlled cylindrical cell for ion storage. A copper jacket surrounding the ion cell can be cooled by flowing liquid nitrogen through coils around the jacket. A total of four thermocouples are mounted near the ion cell. Two thermocouples are in thermal contact with the copper jacket, and two are mounted between the jacket and the ion cell. For experiments in which the cell is cooled, a proportionating controller (Omega Engineering Inc., Stamford, CT) regulates the temperature of the copper jacket by controlling the flow of liquid nitrogen with a solenoid. Experiments at elevated temperature are performed as described previously by heating the entire vacuum chamber using resistive heating blankets on the outside of the chamber.<sup>32</sup> In all cases, experiments are started many hours after the temperature on the controller is set in order to ensure that the radiation field within the ion cell has reached a steady state.

$\text{AA}\cdot\text{M}^+(\text{H}_2\text{O})_1$  clusters are generated by nanoelectrospray ionization. Ions are loaded into the ion cell for 6 s. A shutter is then closed to prevent additional ions from entering the ion cell. A pulse of  $\text{N}_2$  gas ( $2 \times 10^{-6}$  Torr) is used during the load period to help trap the ions. After a 2 s delay, the base pressure in the vacuum chamber returns to  $<5 \times 10^{-9}$  Torr. The ion cluster of interest is isolated using a combination of SWIFT and chirp excitation waveforms. The isolated ions undergo unimolecular dissociation for times ranging from 0.1 to 60 s. The ions are excited for detection using a chirp waveform with a sweep rate of 2200 Hz/ $\mu\text{s}$ . Data are acquired at a rate of 1778 kHz. An Odyssey data system (Finnegan MAT, Bremen, Germany) is used to control the experimental sequence and data acquisition. Dissociation kinetics are obtained by measuring the abundance of the parent and daughter ions as a function of reaction time. For each set of  $\text{AA}\cdot\text{M}^+(\text{H}_2\text{O})_1$  clusters of a particular metal ion (hence the same  $m/z$ ), identical isolation waveforms were used, and kinetic data sets for different AAs were measured immediately following one another.

**Computational Details.** Starting structures for the  $\text{AA}\cdot\text{M}^+$  and  $\text{AA}\cdot\text{M}^+(\text{H}_2\text{O})_1$  clusters, AA = zwitterionic valine (VZ), nonzwitterionic valine (VN), AlaOEt, and Bet, were generated by molecular mechanics and conformational searching using MacroModel (Schrodinger Inc., Portland, OR). A Monte Carlo conformational search using the AMBER\* force field was used to generate 1000 structures. These structures were subsequently energy minimized and clustered into families based on the interactions between the AA, metal ion, and water and on the conformation of the AA backbone. The lowest-energy structure of each family with at least one member conformer within 2.4 kcal/mol (10 kJ/mol) of the minimum-energy conformer was selected for higher level calculations. Additional conformations were selected based on those found previously by other researchers for similar systems<sup>29,31,33</sup> and based on chemical intuition. Hybrid density functional theory (B3LYP) calculations on the selected structures were performed with increasingly large basis sets using Jaguar v. 3.5 and 4.0 (Schrodinger). For clusters with  $\text{M} = \text{Li}$  and  $\text{Na}$ , the basis set progression used was 6-31G\* optimization, followed by 6-31+G\* optimization, followed by single-point energy calculations with the 6-311++G\*\* basis set on the 6-31+G\*-optimized geometry. For

clusters with  $\text{M} = \text{K}$ , the basis sets used were LACVP\*, followed by LACVP+\* and then single-point energy calculations using the LACVP++\*\* basis set at the LACVP+\*-optimized geometry. The LACVP family of basis sets contains an effective core potential to describe the potassium ion and the 6-31G set for other atoms.<sup>34</sup> For several valine-containing conformers, Moller Plesset perturbation theory (MP2) calculations were carried out using GAUSSIAN 98 (Gaussian Inc, Carnegie, PA). Vibrational frequencies and intensities were computed at the RHF/6-31G\* (LACVP\*) level of theory on the lowest-energy  $\text{AA}\cdot\text{M}^+$  clusters to determine zero-point energy and free energy corrections as well as on  $\text{AA}\cdot\text{Li}^+(\text{H}_2\text{O})_1$  clusters for use in master equation analysis.

## Results and Discussion

Structures of  $\text{Val}\cdot\text{M}^+$ ,  $\text{M} = \text{Li}$ ,  $\text{Na}$ , and  $\text{K}$ , and these ions with one water molecule were investigated. Valine was selected for these studies because of the availability of isomeric compounds that ought to be good models for metal ion and water binding to the zwitterion (VZ) and nonzwitterion (VN) forms of valine. Alanine ethyl ester (AlaOEt) and betaine (Bet) were used as models for nonzwitterionic valine and zwitterionic valine, respectively. The structures of these isomers are shown in Scheme 1. VN, VZ, AlaOEt, and Bet will be collectively referred to as AAs (amino acid or amino acid analogues). In the experiments, the rates of water evaporation from valine complexes are compared to those from isomeric complexes of known structure. To infer structural information from these kinetics data, it is critical that the reference compounds (AlaOEt and Bet) are good models for the two forms of valine. There are two basic requirements for this. First, the interaction of the AA, metal ion, and water should be the same in the models and the two forms of valine. We have done extensive modeling, discussed below, to provide strong support that this criterion is met. Second, the activation and dissociation processes of the model compounds must be comparable to those of the two forms of the valine complex. In these experiments, the clusters are activated through the absorption of infrared photons emitted from the vacuum chamber walls. Thus, the compounds must have similar radiative absorption and emission rates. In addition, any differences in the transition state entropies ( $\Delta S^\ddagger$ ) must have minimal effects on the dissociation rates measured for these ions. If radiative absorption and emission rates are comparable, and any differences in  $\Delta S^\ddagger$  result in a minimal effect on the dissociation rate, then the relative dissociation rates of these complexes, measured by blackbody infrared radiative dissociation (BIRD), will reflect differences in binding energy of the water to the  $\text{AA}\cdot\text{M}^+$  complexes. Complexes which coordinate the water and metal ion in the same way should have similar binding energies. Because the water binding in the zwitterion and neutral form of valine differ, it should be possible to distinguish VN vs VZ clusters based on the measured  $\text{AA}\cdot\text{M}^+(\text{H}_2\text{O})_{1-0}$  dissociation kinetics, provided the model compounds meet the criteria above. We have looked at the validity of these assumptions with computations and believe that the models for metal and water binding meet the above-defined criteria. Evidence to support this conclusion is presented in more detail later in the paper.

**Metal Ion Size and Valine Structure.** The location of metal ion attachment to valine depends on the size of the metal ion and whether valine is a zwitterion or nonzwitterion. For  $\text{M} = \text{Li}$ , the structure in which the metal ion is coordinated to both the nitrogen and carbonyl oxygen (NO coordination) of the nonzwitterionic valine is the most stable (NO-coordinated VN,

(32) Price, W. D.; Schnier, P. D.; Williams, E. R. *Anal. Chem.* **1996**, *68*, 859–866.

(33) Lavrich, R. J.; Tubergen, M. J. *J. Am. Chem. Soc.* **2000**, *122*, 2938–2943.

(34) Hay, P. J.; Wadt, W. R. *J. Phys. Chem.* **1985**, *82*, 299–310.

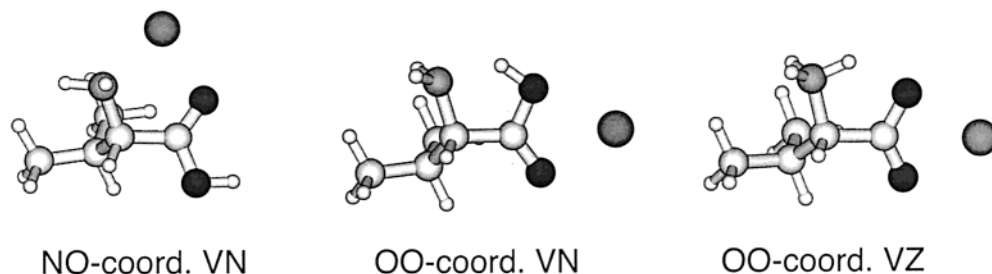


**Figure 1.** Low-energy structures of Val·M<sup>+</sup> complexes illustrated for M = Na.

**Table 1.** Relative Energies of Val·M<sup>+</sup> Complexes at Various Levels of Theory

		$\Delta E$ (kcal/mol)		
		NO-coordinated VN	OO-coordinated VN	OO-coordinated VZ
Li:	B3LYP/6-31G*	0	10.3	2.1
	B3LYP/6-31+G*	0	9.8	1.1
	B3LYP/6-311++G** <sup>a</sup>	0	9.7	3.3
	RHF/6-31G* ZPE <sup>b</sup>	0	-0.9	0.3
	$\Delta G$ (110 °C)	0	-1.3	-0.4
	total <sup>c</sup>	0	7.4	3.2
Na:	B3LYP/6-31G*	0.7	3.9	0
	B3LYP/6-31+G*	1.8	4.5	0
	B3LYP/6-311++G** <sup>a</sup>	0	3.0	0.9
	MP2/6-31G*	1.6	5.3	0
	MP2/6-31+G*	2.9	6.0	0
	MP2/6-311++G** <sup>a</sup>	0	2.9	1.6
	RHF/6-31G* ZPE <sup>b</sup>	0	-0.5	0.5
	$\Delta G$ (30 °C)	0	-0.7	-0.2
	total <sup>c</sup>	0	1.8	1.2
K:	B3LYP/LACVP*	1.8	0	1.1
	B3LYP/LACVP+*	2.3	0.4	0
	B3LYP/LACVP++** <sup>a</sup>	0.5	0	1.5
	RHF/LACVP* ZPE <sup>b</sup>	0.4	0	0.9
	$\Delta G$ (-10 °C)	0.7	0	0.6
	total <sup>c</sup>	1.6	0	3.0

<sup>a</sup> Single-point energy calculation. <sup>b</sup> Zero-point energy correction. <sup>c</sup>  $\Delta E$  (B3LYP/biggest basis set + ZPE + G).

Figure 1 left). The nonzwitterion structure in which the metal ion coordinates to both oxygens of the carboxylic group (OO-coordinated VN middle) is  $\sim 7$  kcal/mol less stable (Table 1). In the zwitterion form, the metal binds to both oxygens of the carboxylate group (OO coordinated VZ right). This structure is only slightly (1–3 kcal/mol) higher in energy than NO-coordinated VN at all levels of theory used. For M = Na, the NO-coordinated VN and OO-coordinated VZ are comparable in energy, with the VN form slightly favored at the highest level of theory. The OO-coordinated VN is still higher in energy than either of the other two forms, but this difference is less than that with Li. For M = K, the NO-coordinated VN is less stable than the OO-coordinated VN. Thus, the favored position of the metal ion in VN changes from NO coordination to OO coordination with increasing metal ion size. At the highest levels of theory, the nonzwitterionic form of valine is 1–3 kcal/mol more stable than the zwitterionic form for all M investigated.

Similar results have been reported for Gly·M<sup>+</sup>.<sup>9–11</sup> For M = Li and Na, NO coordination of nonzwitterionic glycine is favored, but the OO- and NO-coordinated structures are degenerate for K. For M = Rb and Cs, OO coordination of the metal ion is the most stable. For all of the alkali metal ions, there is a stable complex in which zwitterionic glycine interacts with the metal by OO coordination. The zwitterion-containing conformer is found to be less stable than the lowest-energy nonzwitterion-containing conformer of Gly·M<sup>+</sup> by 1–3 kcal/

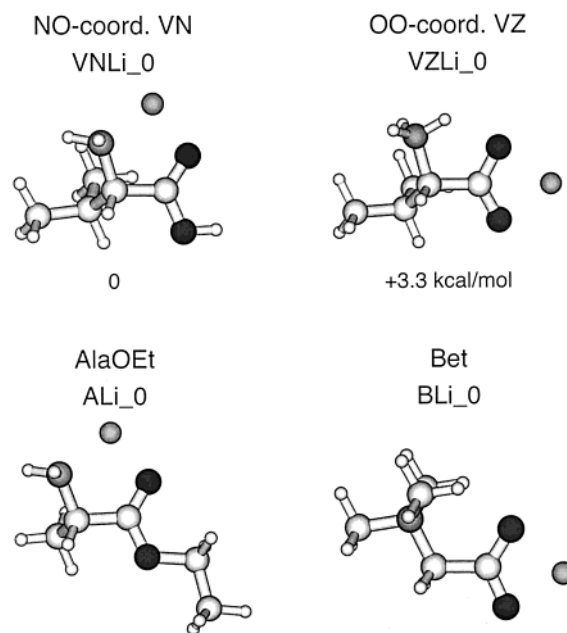


**Figure 2.** Lowest-energy structures for AA·Li<sup>+</sup> complexes. The identity of the AA is labeled on the figure. Relative energies for the AA = Val complexes are from single-point energy calculations at the B3LYP/6-311++G\*\* level using the B3LYP/6-31+G\*-optimized geometry.

mol, similar to the energy difference found for Val·M<sup>+</sup> conformers.

Hoyau and Ohanessian have calculated the barrier for conversion between the Gly·Na<sup>+</sup> structures. The barrier for conversion between NO- and OO-coordinated structures is substantial,  $\sim 20$  kcal/mol. In contrast, the barrier for conversion between OO-coordinated VN and OO-coordinated VZ is extremely small, 2 kcal/mol along the potential energy surface and zero when zero-point vibrational energy corrections are included.<sup>10</sup> Assuming similar barriers exist in our experiments, we may reasonably hope to distinguish NO and OO coordination, but probably not VN OO coordination vs VZ OO coordination.

**Structures of Cationized Analogues.** Extensive computational work was done on all compounds in order to determine if the models for the two forms of valine have similar metal ion–AA–water molecule interactions. For the sake of clarity, only the lowest-energy structures found will be discussed here. A more extensive discussion of the variety of structures that were identified is presented later. Figure 2 shows the lowest-energy conformers for AA·Li<sup>+</sup>, AA = VN, VZ, AlaOEt, and Bet. The lowest-energy Val·Li<sup>+</sup> structure is the nonzwitterionic form with NO-coordinated metal ion (Figure 2, VNLi\_0, which stands for valine nonzwitterion coordinated to lithium with 0 waters attached). By far, the lowest-energy structure for AOEt·Li<sup>+</sup> is one in which the lithium ion is also NO-coordinated

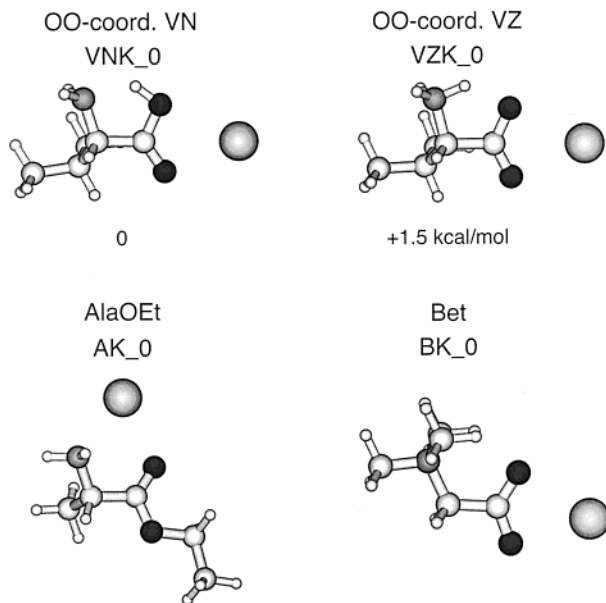


**Figure 3.** Lowest-energy structures for  $AA \cdot K^+$  complexes. The identity of the AA is labeled on the figure. Relative energies for the AA = Val complexes are from single-point energy calculations at the B3LYP/LACVP++\*\* level using the B3LYP/LACVP+\*-optimized geometry.

(ALi\_0, Figure 2). The  $Li^+$ -AA interaction is essentially the same in both of these structures. Nearly identical structures are obtained for Na, but the AA- $M^+$  bond distance is slightly longer. Thus, AlaOEt appears to be a very good structural model of VN with  $M = Li$  and Na.

For  $VZ \cdot M^+$ , there is only one competitive structure, labeled VZLi\_0 in Figure 2. The metal ion-AA interaction appears to be well-mimicked by the Bet- $Li^+$  isomer, BLi\_0. Again, structures for  $M = Na$  are virtually identical to those shown for  $M = Li$ . Thus, AlaOEt and Bet have essentially the same interactions with  $Li^+$  and  $Na^+$  as do VN and VZ, respectively.

The lowest-energy conformers found for  $AA \cdot K^+$  are shown in Figure 3. Both VNK\_0 and VZK\_0 have an OO-coordinated metal ion. These two conformations differ by only a simple proton transfer. VNK\_0 is more stable than VZK\_0 by 1.5 kcal/mol at the highest level of theory used. With zero-point energy and thermal corrections, this difference increases to 3.0 kcal/mol (Table 1). Bet- $K^+$  also has an OO-coordinated potassium ion, and this interaction is very similar to that in VZK\_0. This indicates that it is a good structural model for VZ. However, AlaOEt- $K^+$  has a NO-coordinated metal ion and does not resemble VNK\_0. Thus, it is not a suitable model for VNK\_0.

**Mode of Water Binding.** The lowest-energy conformers for  $AA \cdot Li^+(H_2O)_1$  are shown in Figure 4. For AA = VN and AlaOEt, the water molecule attaches to the NO-coordinated metal ion and has no direct interaction with the AA. For these isomers, the structures shown in Figure 4 are essentially equivalent to the  $AA \cdot Li^+$  conformers shown in Figure 2. Thus, the addition of a single water molecule does not have a significant effect on the structure of any of the nonzwitterionic  $AA \cdot M^+$  complexes. For the VZ cluster, the conformer shown is degenerate (within 0.2 kcal/mol at the highest level of theory) with one closely resembling BLi\_1 in which the metal ion is evenly shared between the oxygens of the carboxylate group, and the water is bound only to the metal ion (VZA, Figure 5; the relative energies on the figure are at a lower level to compare the large number of conformers investigated). Under the conditions of the experiment, both of the conformations are almost certainly present and rapidly interconverting. Both VZ

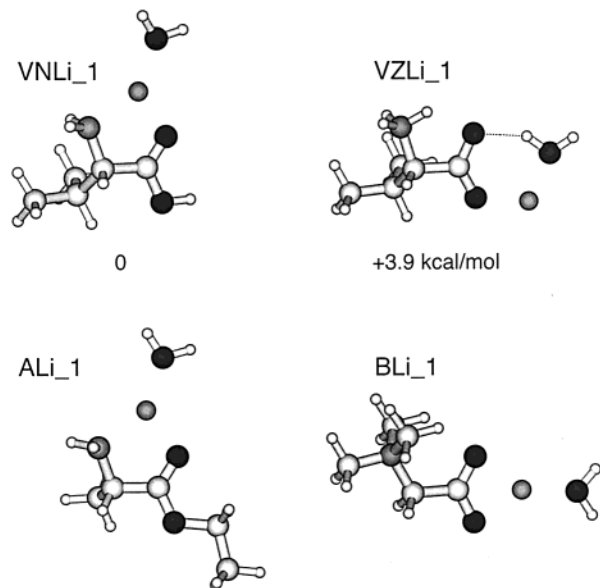


**Figure 4.** Lowest-energy structures for  $AA \cdot Li^+(H_2O)_1$  complexes. Relative energies for the AA = Val complexes are from single-point energy calculations at the B3LYP/6-311++G\*\* level on the B3LYP/6-31+G\*-optimized geometry.

conformers are still  $\sim 4$  kcal/mol higher in energy than the VN-containing cluster at the B3LYP/6-311++G\*\* level of theory (Table 2). These results indicate that the Val- $Li^+$ -water interactions in VN and VZ are well-simulated by the model compounds AlaOEt and Bet, respectively. It is also clear from the calculations that the addition of a single water molecule does not stabilize the VZ-containing conformer relative to the VN-containing conformer.

The lowest-energy conformers of  $AA \cdot Na^+(H_2O)_1$  are similar to those shown for  $M = Li$  in Figure 4. Again, the VZ conformer shown is nearly degenerate with an alternative form in which the water is bound solely to the metal ion. For  $M = Na$ , the VN structure is  $\sim 2$  kcal/mol more stable than the VZ structure. As was found for the lithiated clusters, the lowest-energy structures found for the  $AA \cdot Na^+(H_2O)_1$  compounds indicate that the metal ion-AA-water interaction of the VN- and VZ-containing clusters is well-mimicked by the AlaOEt- and Bet-containing clusters, respectively.

Figure 6 shows the structures of potassiumated clusters with one water molecule attached. In all cases, the water molecule in the lowest-energy structure interacts with the metal ion and also forms a hydrogen bond to the AA. As is the case without water (Figure 3), VNK\_1 and VZK\_1 closely resemble each other, differing by a simple proton transfer. The Val- $K^+$ -water interaction in VNK\_1 looks identical to that in BK\_1. AK\_1 does not appear to be a good model for VNK\_1. At the highest level of theory used, VNK\_1 is more stable than VZK\_1 by 1.4 kcal/mol. Thus, the addition of a water molecule has no effect on the relative energies of the VN and VZ complexes with K.

Overall, the structures shown in Figures 1-4 and 6 indicate that AlaOEt and Bet model well the VN and VZ interactions with  $Li^+$  and  $Na^+$ . Bet is also a good structural model for VZ with  $K^+$ . However, AlaOEt does not provide a good model for the VN- $K^+$  interaction. In fact, the VN- $K^+$  interactions may be similar to the Bet- $K^+$  interactions.

**Kinetic Data.** The relative blackbody dissociation kinetics for the loss of one water molecule,  $AA \cdot M^+(H_2O)_1 \rightarrow 0$ ,  $M = Li, Na, \text{ and } K$ , are shown in Figure 7. These data were acquired at

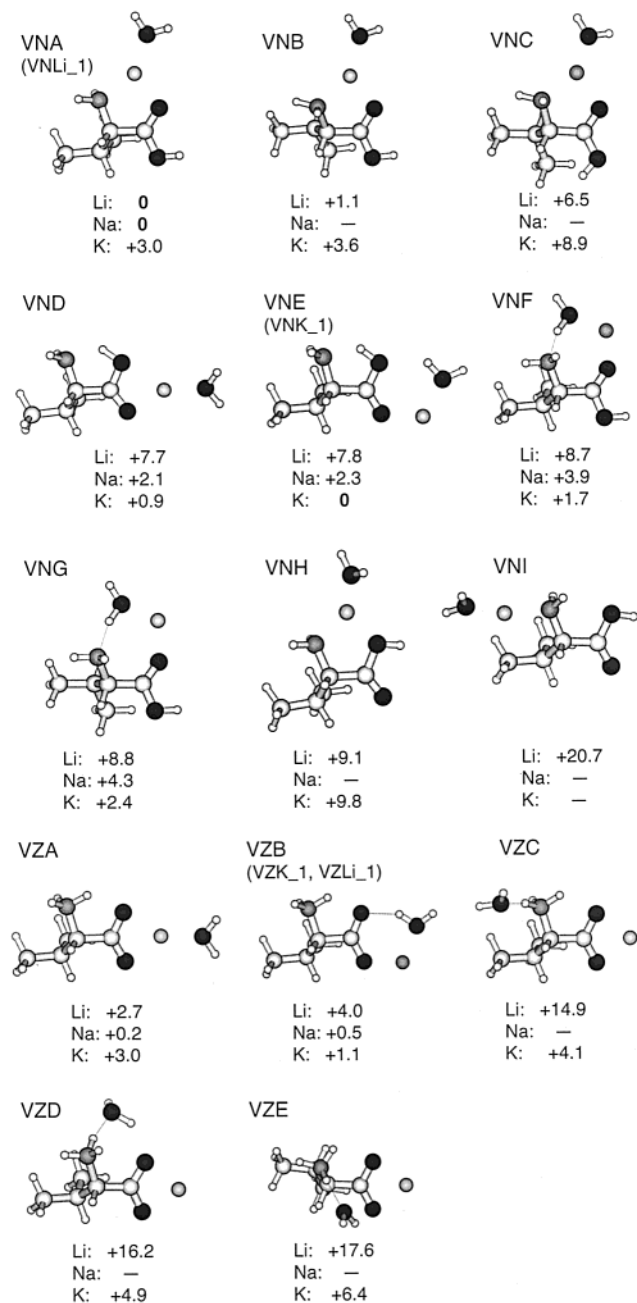


**Figure 5.** B3LYP/6-31G\*-optimized structures and relative energies (kcal/mol) for Val·M<sup>+</sup>(H<sub>2</sub>O)<sub>1</sub> clusters. Note that the relative energies of some of these structures changes for the subsets calculated at higher levels of theory (see text).

a temperature of +110, +30, and −10 °C, for Li, Na, and K, respectively. The kinetic plots show the natural log of the normalized abundance of the precursor ion,  $\ln\{[AA\cdot M^+(H_2O)_1]/([AA\cdot M^+(H_2O)_1] + [AA\cdot M^+])\}$ , as a function of reaction time. All the data can be fit well by straight lines (correlation coefficients > 0.998), indicating first-order kinetics. The measured dissociation rates of each complex are given in Table 3. As the size of M<sup>+</sup> increases, the temperature necessary to obtain similar AA·M<sup>+</sup>(H<sub>2</sub>O)<sub>1</sub> dissociation rates decreases. This trend mirrors that in M<sup>+</sup>(H<sub>2</sub>O)<sub>n</sub> cluster-binding energies<sup>35</sup> and is presumably due to the lower binding energy of water with increasing metal ion size.

For AA·Li<sup>+</sup>(H<sub>2</sub>O) (Figure 7a), dissociation of the Val cluster is much more similar to the AlaOEt cluster (~14% difference)

than to the Bet cluster (~56% difference). Because the dissociation of valine is more similar to AlaOEt, which is the model for the neutral structure, this result indicates that the structure of Val is nonzwitterionic. If Val were zwitterionic, the dissociation rate should have been closer to that of Bet, the model of the zwitterion. Similar results are obtained for M = Na (Figure 7b), again suggesting that valine is nonzwitterionic in these clusters.

For M = K, a very different result is observed. The dissociation rates of Val·K<sup>+</sup>(H<sub>2</sub>O)<sub>1</sub> and Bet·K<sup>+</sup>(H<sub>2</sub>O)<sub>1</sub> are very close (~7% difference), while the dissociation of AlaOEt·K<sup>+</sup>(H<sub>2</sub>O)<sub>1</sub> is significantly faster (~44% difference). These data suggest that water binding to Val·K<sup>+</sup> and Bet·K<sup>+</sup> is similar. This result indicates that the metal ion in Val·K<sup>+</sup> must be OO coordinated. However, it is not possible to differentiate between an OO-coordinated VN or VZ structure based on these results alone. The OO-coordinated VN and VZ structures differ only by the position of the acidic hydrogen. The barrier (if any) between these structures is expected to be much lower than the barrier for water loss. Thus, these structures likely interconvert under the conditions of the BIRD experiment. These kinetic data are consistent with the lowest-energy structures calculated for the potassiumated cluster (Figures 3 and 6), which indicate that the water binding in VNK, VZK, and BK are similar, but are dissimilar to water binding in AK.

**Calculated Binding Energies.** To assess whether the differences in the measured rate constants between the isomers are consistent with the strength of the interaction of the water molecule with each of these isomers, binding energies were determined using the lowest energy structures for each AA·M<sup>+</sup> and AA·M<sup>+</sup>(H<sub>2</sub>O) at the B3LYP/6-31+G\* level of theory (LACVP+\* for M = K). Binding energies from subsequent single point calculations at the B3LYP/6-311++G\*\* level (LACVP++\*\* for M = K) are given in Table 4. The binding energies consistently decrease with increasing level of theory, indicating that the true binding energies could be even lower. However, the relative ordering of binding energies of AA·Li<sup>+</sup>(H<sub>2</sub>O) do not depend on the level of theory used here.

These calculated binding energies indicate that, all else being equal, the ordering of stability of AA·Li<sup>+</sup>(H<sub>2</sub>O) follows the trend: VN > VZ ≈ AlaOEt > Bet. This result is consistent with the ordering of the measured rate constants. To validate the comparison between calculated binding energies and measured kinetic data at one temperature, the effects of radiative absorption and emission as well as transition state entropy must be determined. These effects are modeled in the following section.

**Activation and Dissociation Processes.** Structural information inferred from these kinetic data depend on our having model structures in which the water binding is similar and for which the photoactivation/deactivation rates are similar to the valine-containing ions. Here, we discuss how any differences in radiative rates and dissociation entropies for these isomers would effect the observed dissociation kinetics. In these experiments, the measured dissociation rate depends on the rates of radiative absorption and emission, the transition-state entropy of the dissociation, and the binding energy of the water to the ion. We can numerically simulate the experiment by modeling these processes using a master equation formalism. This is discussed in detail elsewhere.<sup>36,37</sup> Briefly, radiative rates are obtained by combining Einstein coefficients determined from calculated

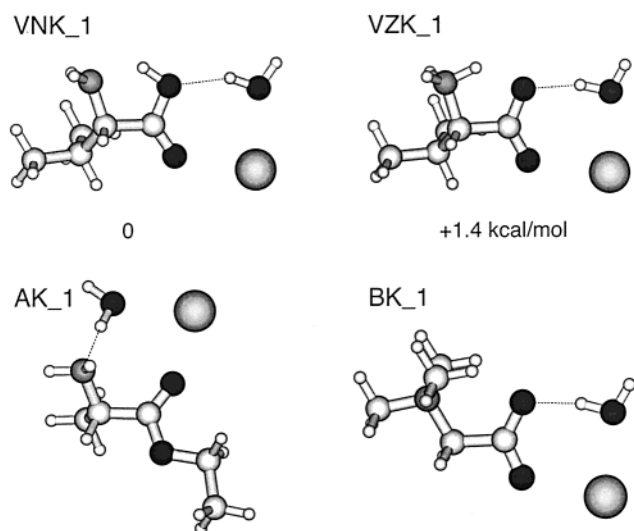
(36) Price, W. D.; Schnier, P. D.; Williams, E. R. *J. Phys. Chem. B* **1997**, *101*, 664–673.

(37) Jockusch, R. A.; Williams, E. R. *J. Phys. Chem. A* **1998**, *102*, 4543–4550.

(35) Dzidic, I.; Kebarle, P. *J. Phys. Chem.* **1970**, *74*, 1466–1474.

**Table 2.** Relative Energies, in Kilocalories per Mole, of Selected Val·M<sup>+</sup>(H<sub>2</sub>O)<sub>1</sub> Conformations at Various Level of Theory

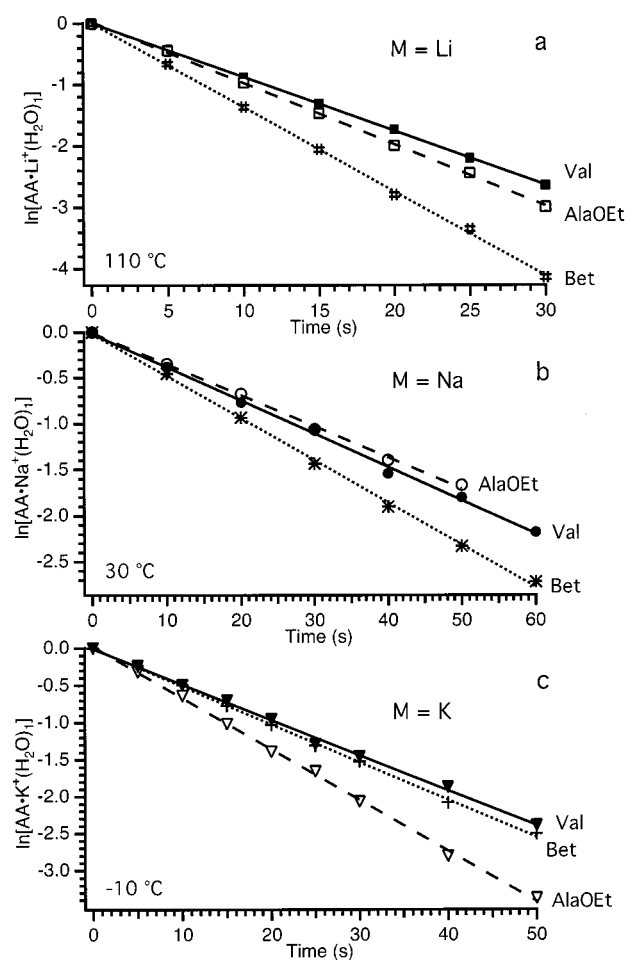
M	method/basis set	VNA (VNLI_1)	VND	VNE (V NK_1)	VNG	VZA	VZB (VZM_1)
Li:	B3LYP/6-31G*	0	7.7	7.8	8.8	2.7	4.0
	B3LYP/6-31+G*	0	7.2	6.7	7.9	1.6	2.3
	B3LYP/6-311++G** <sup>a</sup>	0	7.3	6.1	7.8	4.1	3.9
Na:	RHF/6-31 G*	0	4.6	4.9	6.6	5.3	7.0
	B3LYP/6-31G*	0	2.1	2.3	4.3	0.2	0.5
	B3LYP/6-31+G*	1.4	3.1	2.6	4.4	0.5	0
	B3LYP/6-311++G** <sup>a</sup>	0	3.4	0.2	4.7	2.6	2.0
	MP2/6-31 G*	0.5	3.5	3.9	5.5	0	0.8
	MP2/6-31 +G*	2.1	4.3	3.8	5.1	0.1	0
	MP2/6-31 1++G** <sup>a</sup>	0	2.0	1.1	2.8	2.2	1.9
K:	B3LYP/L ACVP*	3.0	0.9	0	2.4	3.0	1.1
	B3LYP/L ACVP+*	4.1	1.9	0.4	2.7	2.8	0
	B3LYP/L ACVP++* <sup>a</sup>	3.5	1.1	0	2.6	3.6	1.4

<sup>a</sup> Single-point energy calculation.**Figure 6.** Lowest-energy structures for AA·K<sup>+</sup>(H<sub>2</sub>O)<sub>1</sub> complexes. Relative energies for the AA = Val complexes are from single-point energy calculations at the B3LYP/LACVP++\*\* level on the B3LYP/LACVP+\*-optimized geometry.

absorption spectra for the clusters and a blackbody energy field at the temperature of the experiment. Dissociation processes are included in the model by using microcanonical rate constants calculated with RRKM theory. Typically, the transition-state entropy of the dissociation is not known, so we model a range of transition-state entropies which results in a range of dissociation rate constants. The binding energy used to calculate the RRKM rate constants can also be varied in the model.

Figure 8 shows the calculated absorption spectra for the lowest-energy conformers of each of the AA·Li<sup>+</sup>(H<sub>2</sub>O)<sub>1</sub> clusters overlaid by a blackbody field at 110 °C (the temperature of the experiments). Qualitatively, the absorption spectra for the nonwitterion-containing clusters (ALi\_1 and VNLI\_1) closely resemble each other, as do those of the zwitterion-containing clusters (BLi\_1 and VZLi\_1). Thus, the radiative processes for the model compounds appear to be very similar to the valine-containing clusters they are meant to model.

Master equation modeling was done using these calculated absorption spectra in order to assess the effect of radiative rates and transition state entropy in a more quantitative manner. Table 5 shows the dissociation rates for the lithiated clusters calculated using the master equation model at 110 °C for each of the isomers assuming both a “neutral” and “loose” transition state (Arrhenius preexponentials of 10<sup>13</sup> and 10<sup>18</sup> s<sup>-1</sup>, respectively) and a bond dissociation energy of 0.85 eV. Dissociation of water from these clusters should go through a relatively loose transition

**Figure 7.** Blackbody infrared dissociation kinetics for the evaporation of water from AA·M<sup>+</sup>(H<sub>2</sub>O)<sub>1</sub> clusters for M = Li (a), Na (b), and K (c). The temperature at which the experiments were done is labeled on the figure.

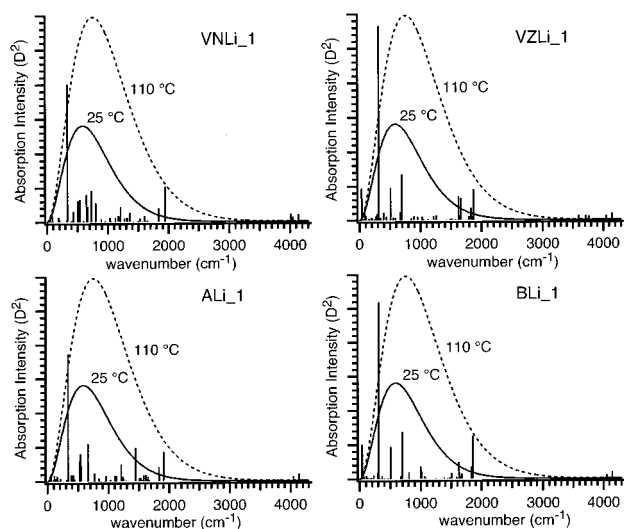
state, but a wider range was used to better assess the effect of this parameter. A threshold dissociation energy ( $E_0$ ) of 0.85 eV roughly reproduces the measured rate for Val·Li<sup>+</sup>(H<sub>2</sub>O)<sub>1</sub>→<sub>0</sub> measured at 110 °C. This value is lower than the calculated binding energy of 1.11 eV. Even by multiplying the calculated transition dipole moments by two and by using an Arrhenius preexponential of 10<sup>17</sup> s<sup>-1</sup>, the maximum value of  $E_0$  that gives a rate constant within a factor of 2 of the measured value is 1.02 eV. As noted earlier, the calculated binding energies consistently decrease with increasing level of theory used. In addition, single point calculations were performed on just one low-energy conformer of AlaOEt and Bet selected at a low level

**Table 3.** Measured Dissociation Rates for  $AA \cdot M^+(H_2O)_{1-0}$  (Error Corresponds to the Standard Deviation of the Linear Least-Squares Best Fit Line)

M	AA	rate ( $s^{-1}$ )	% difference
Li	Val	$0.0879 \pm 0.0005$	
	AlaOEt	$0.0999 \pm 0.0010$	+13.7%
Na	Bet	$0.1372 \pm 0.0016$	+56.1%
	Val	$0.0366 \pm 0.0011$	
	AlaOEt	$0.0339 \pm 0.0007$	-7.4%
K	Bet	$0.0460 \pm 0.0008$	+26%
	Val	$0.0476 \pm 0.0009$	
	AlaOEt	$0.0688 \pm 0.0009$	+44.5%
	Bet	$0.0510 \pm 0.0006$	+7.1%

**Table 4.** Binding Energies of Water for  $AA \cdot M^+(H_2O)_1$  from Density Functional Calculations at the B3LYP/6-311++G\*\* Level of Theory (B3LYP/LACVP++\*\* for  $M = K$ )

conformer	binding energy (eV)	conformer	binding energy (eV)
VNLI_1	1.11	VNNA_1	0.88
VZLI_1	1.08	VZNA_1	0.84
ALi_1	1.08	VNK_1	0.70
BLi_1	1.04	VZK_1	0.59

**Figure 8.** Planck distributions at 110 and 25 °C overlaying calculated radiative absorption intensities ( $D^2$ ) for the lowest energy  $AA \cdot Li^+(H_2O)_1$  complexes shown in Figure 4. Vertical axes have arbitrary units but remain constant for all isomeric clusters.

of theory, so an even lower energy structure for these isomers could be present. Finally, by far the best way to extract values of  $E_0$  from the measured kinetic data is by modeling data measured over a wide range of temperatures. These measurements are currently underway. For comparison, a bond dissociation energy of 0.97 eV has been measured by Rogers and Armentrout for  $Li^+(H_2O)_{3-2}$ .<sup>38</sup>

Table 5 also lists the percent change in rate compared to VNLI\_1 or, in the case of the measured experimental rates, percent change in comparison to  $Val \cdot Li^+(H_2O)_1$ . The calculated dissociation rates do depend slightly on the structure of the ion, indicating that these ions absorb and emit photons at slightly different rates. The calculated rates for the nonzwitterion clusters are higher than those for the zwitterion clusters. Within the nonzwitterion clusters, the model compound ALi\_1 dissociates ~10% faster than VNLI\_1, even though these clusters are modeled with the same bond dissociation energy. This calculated

**Table 5.** Comparison of Dissociation Rates for  $AA \cdot Li^+(H_2O)_{1-0}$  (Calculated Values Are from Master Equation Model Assuming a Bond Dissociation Energy of 0.85 eV)

conformer	calcd				measd	
	neutral transn state		loose transn state			
	rate ( $s^{-1}$ )	% change	rate ( $s^{-1}$ )	% change	rate ( $s^{-1}$ )	% change
VNLI_1	0.0725		0.108		0.0879	
VZLI_1	0.0693	-4.5%	0.105	-3.0%		
ALi_1	0.0784	+8.1%	0.119	+10%	0.0999	+13.7%
BLi_1	0.0622	-14%	0.0912	-16%	0.1372	+56.1%

difference in dissociation rates is approximately the same as the measured difference for these isomers. However, this agreement may be fortuitous; the accuracy of individual absorption intensities calculated at the RHF/6-31G\* level is not well-characterized, although we and others have found that the integrated intensities are approximately correct.<sup>36,39</sup> The calculated dissociation rate of BLi\_1 is ~10–15% slower than VZLI\_1 or VNLI\_1. However, the experimentally measured dissociation rate is *over 50% faster* than that of  $Val \cdot Li^+(H_2O)_1$ . This difference in experimentally measured rates is significantly larger than the variation calculated due to difference in just the radiative absorption and emission rates.

The master equation modeling results shown in Table 5 also address the effect of transition-state entropy on the dissociation rate. Because the model clusters bind the metal and water in the same way as the Val-containing clusters, it is likely that they will have very similar transition states and transition-state entropies to the forms of valine they are meant to model. In addition, dissociation of water should have a fairly “loose” transition state, much looser than the neutral transition state modeled here with an Arrhenius preexponential factor of  $10^{13} s^{-1}$ . What is presented here is a worst-case scenario. Even if  $Val \cdot Li^+(H_2O)_1$  (VZLI\_1 or VNLI\_1) dissociates via a neutral transition state and BLi\_1 dissociates via a loose transition state, the calculated maximum difference in rates is 32%. The 56% difference in measured rates cannot be accounted for just by differences in radiative absorption/emission rates or transition-state entropy. *Instead, this large difference in measured rates indicates that the binding energy of water in these clusters is different.* Water is more tightly bound to  $Val \cdot Li^+(H_2O)$  and  $AlaOEt \cdot Li^+(H_2O)$  than to  $Bet \cdot Li^+(H_2O)$ . This result is consistent with the relative binding energies determined from theory (Table 4). Taken together, our experimental and computational results clearly indicate that  $Val \cdot Li^+(H_2O)$  contains nonzwitterionic valine which has an NO-coordinated metal ion; i.e., it adopts a VNLI\_1-like structure.

The measured dissociation rate increases with increasing metal ion size. The overall radiative rates should not change much with metal ion size. Thus, this trend is presumably due to a decrease in water-binding energy with metal ion size. Therefore, as the size of the metal ion increases, the dissociation process moves closer to the truncated Boltzmann regime. In this regime, the dissociation rate is determined by radiative absorption rates and by the dissociation energy and is not effected by  $\Delta S^\ddagger$ .<sup>40</sup> Thus, the transition-state entropy should play a smaller role in determining the dissociation rate of the clusters with larger M. Absorption spectra have not been calculated for the clusters with  $M = Na$  and  $K$ , but it is reasonable to expect that these will closely resemble each other, as is the case for M

(38) Rodgers, M. T.; Armentrout, P. B. *J. Phys. Chem. A* **1997**, *101*, 1238–1249.(39) Dunbar, R. C.; McMahon, T. B.; Tholmann, D.; Tonner, D. S.; Salahub, D. R.; Wei, D. *J. Am. Chem. Soc.* **1995**, *117*, 12819–12825.(40) Dunbar, R. C. *J. Phys. Chem.* **1994**, *98*, 8705–8712.

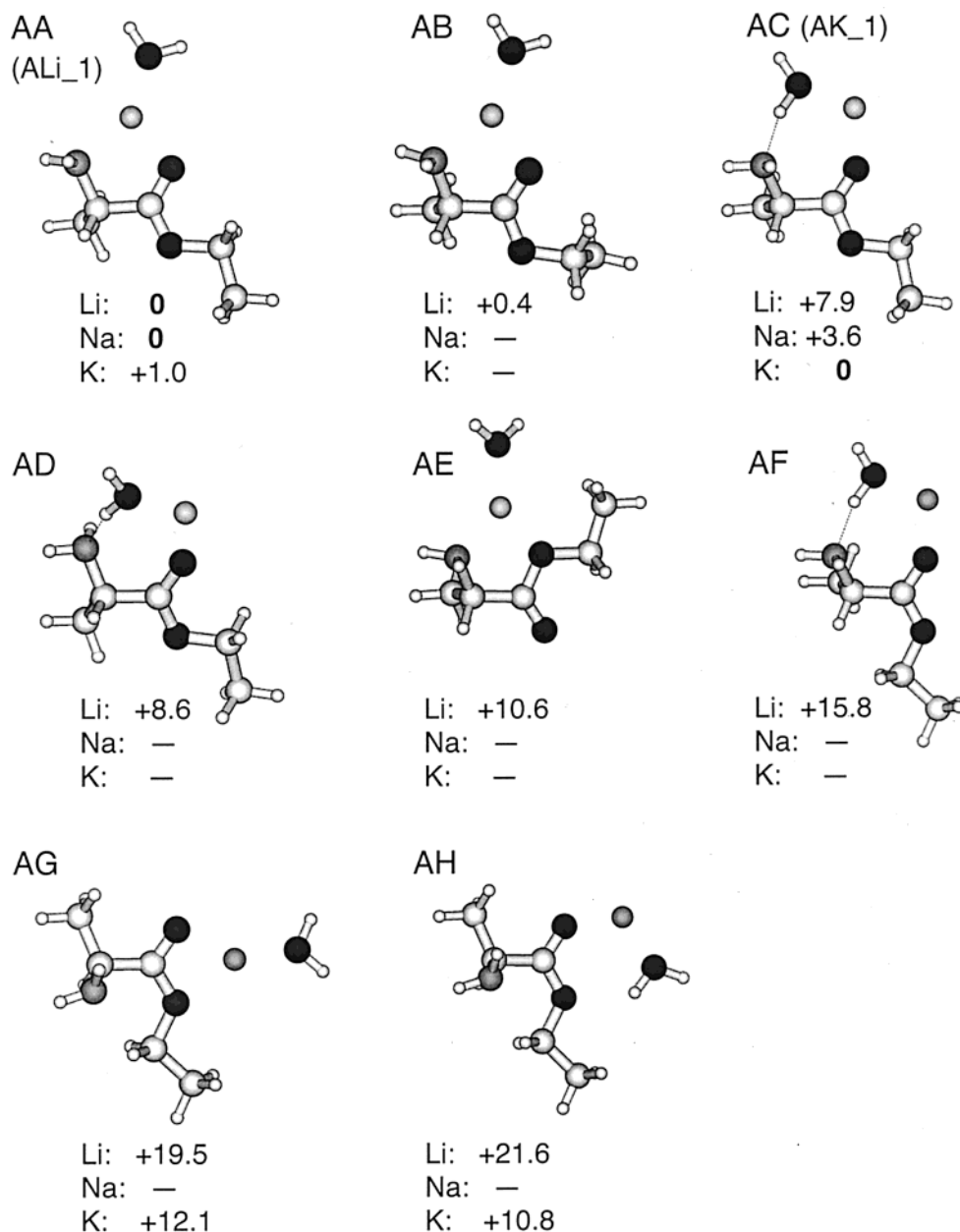


**Figure 9.** B3LYP/6-31G\*-optimized structures and relative energies (kcal/mol) for AlaOEt·M<sup>+</sup>(H<sub>2</sub>O)<sub>1</sub> clusters.

= Li. Thus, the relative dissociation kinetics for M = Na and K (Figure 7 and Table 3) should reflect the relative binding energies of the isomeric clusters even more closely than for M = Li. These results strongly suggest that Val·Na<sup>+</sup>(H<sub>2</sub>O)<sub>1</sub> contains nonzwitterionic valine which chelates the sodium ion in an NO fashion. Val·K<sup>+</sup>(H<sub>2</sub>O) appears to have OO coordination of the metal ion, but the zwitterionic vs nonzwitterionic nature of the valine cannot be determined from this experiment.

**Other Structures and Trends.** Even with only one water molecule, there are many different AA·M<sup>+</sup>(H<sub>2</sub>O)<sub>1</sub> conformers that are stable, some of which are close in energy to the lowest-energy conformer identified. Figures 5, 9, and 10 show many of the conformations that were investigated in order to illustrate the range of conformation space which was searched to find the low-energy conformers shown in Figures 2–4 and 6. Figure 5 shows most of the B3LYP/6-31G\*-optimized structures that were identified for Val·Li<sup>+</sup>(H<sub>2</sub>O). The relative energies of these conformers, as well as similar conformers found for M = K (optimized at the B3LYP/LACVP\* level) are listed in the figure. In all low-energy conformations, the metal ion is chelated by

the electronegative oxygens and/or nitrogen. Several of the conformers are stabilized by hydrogen bonds, either within the Val or between the Val and the water molecule.

Several trends are apparent. For small metal ions, NO coordination is energetically favored over OO coordination (e.g., VNA, VNB, and VNC vs VND). This is likely due to the ability of the NO-coordination geometry to surround small charges vs the more rigid geometry of the carboxylic acid group. Also, the position of the side chain (or nonpolar groups in general) has only a minor effect on the energy of the conformation (e.g., VNA vs VNB, VNF vs VNG, AA vs AB). Instead, two factors are of primary importance. First is the maximization of electrostatic interactions, which is particularly important for the small metal ions. Second is the insertion of water to form a hydrogen bond with the AA, which is increasingly important for the larger metal ions. For example, water insertion in the NO-coordinated nonzwitterionic valine does not occur for lithium and sodium but does for potassium (VNA for Li and Na, vs VNF for K). Similarly, water insertion in the OO-coordinated valine is favorable for all metals, but only margin-

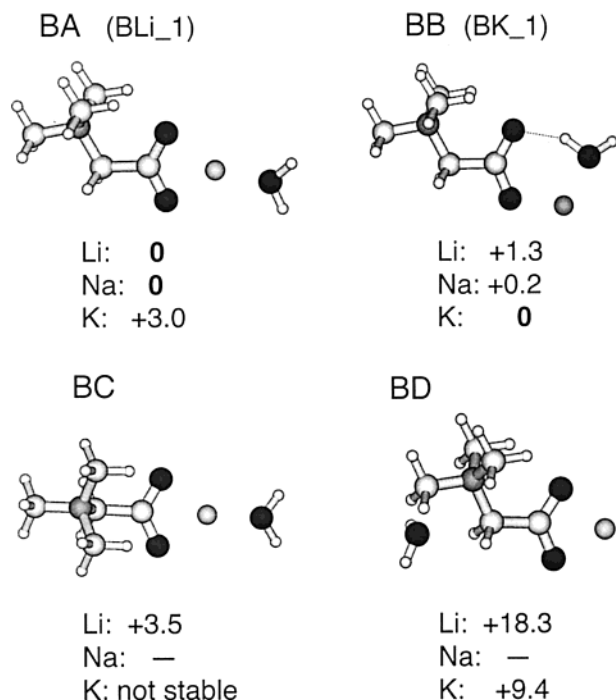


**Figure 10.** B3LYP/6-31G\*-optimized structures and relative energies (kcal/mol) for  $\text{Bet}\cdot\text{M}^+(\text{H}_2\text{O})_1$  clusters.

ally so for lithium, and significantly so for potassium (e.g., VND vs VNE, VZA vs VZB). These results are consistent with a smaller interaction energy between the AA and potassium vs lithium, making the hydrogen bond more important in the potassiumated structure.

Figures 5, 9, and 10 also illustrate the cases in which the AlaOEt and Bet are good structural models for VN and VZ. Examining the range of VN conformations found, it is apparent that any conformation which does not specifically involve the hydroxyl forming an intramolecular hydrogen bond can be well-modeled by AlaOEt (e.g., VNA and AA, VNF and AC, VNH and AE). Any conformations in which this hydrogen bond is present look similar to VZ and Bet (e.g., VND is similar to VZA and BA, not to AG). Any VZ cluster in which the water and metal ion interact solely with the carboxylate group of the zwitterion has an essentially analogous Bet cluster (VZA and BA, VZB and BB). The relative energies of these types of interactions also remain relatively constant (e.g., the energy difference between VZA and VZB compared to BA and BB). Bet, with bulky methyl groups attached to the nitrogen, is not a good model for conformations in which the water bonds to the protonated N-terminus or bridges between this and the carboxylate group, as in VZC, VZD and VZE. However, it is not energetically favorable to attach the water molecule to the  $\text{VZ}\cdot\text{M}^+$  cluster in this way, particularly for the small  $\text{M}^+$ .

## Conclusions

Results from both theory and experiment indicate that the mode of metal ion binding in  $\text{Val}\cdot\text{M}^+$  complexes changes with the size of the metal ion. Calculations show that the lowest-energy structures of  $\text{Val}\cdot\text{Li}^+$  and  $\text{Val}\cdot\text{Li}^+(\text{H}_2\text{O})_1$  have the lithium ion chelated by the nitrogen and carbonyl oxygen of non-zwitterionic valine. The measured relative dissociation kinetics for  $\text{AA}\cdot\text{Li}^+(\text{H}_2\text{O})_{1-0}$  are in agreement with results from theory. For  $\text{M} = \text{Na}$ , the results of high-level calculations are not in agreement with the prediction of Bowers and co-workers that  $\text{Val}\cdot\text{Na}^+$  forms a salt-bridge structure.<sup>17</sup> At the MP2/6-

311++G\*\* level, including RHF/6-31G\* zero-point and free-energy corrections, a structure in which the sodium ion is NO-coordinated to nonzwitterionic valine is lower in energy than the OO-coordinated zwitterion structure by 1.9 kcal/mol. The measured dissociation kinetics of  $\text{AA}\cdot\text{Na}^+(\text{H}_2\text{O})_{1-0}$  clusters are consistent with this structure. The experimental results indicate that  $\text{Val}\cdot\text{Na}^+(\text{H}_2\text{O})_1$  has NO coordination of the metal ion to a nonzwitterionic valine, thus forming a charge-solvated structure. For  $\text{M} = \text{K}$ , theory predicts that OO coordination of the metal ion is favored over NO coordination, although the difference in energy between structures is relatively small (2.6 kcal/mol). Relative dissociation kinetics of  $\text{AA}\cdot\text{K}^+(\text{H}_2\text{O})_{1-0}$  also suggest that potassium is OO-coordinated to valine, but we are unable to distinguish if the valine is zwitterionic or nonzwitterionic from these experiments alone.

Calculations reported here indicate that the addition of a single water molecule to  $\text{Val}\cdot\text{M}^+$  does not significantly effect the relative energetics of structures containing zwitterionic and nonzwitterionic valine. For  $\text{M} = \text{Li}$ , the water simply coordinates to the metal ion, leaving the  $\text{Val}\text{-Li}^+$  interaction virtually unchanged. For  $\text{M} = \text{K}$ , the water is hydrogen bonded to the Val as well as coordinated to the metal ion in the lowest-energy structures. This difference in water coordination with size of metal ion reflects the strength of the  $\text{AA}\text{-M}^+$  interaction compared to an  $\text{AA}\text{-water}$  (hydrogen bonding) interaction. For the smaller metal ion, the electrostatic  $\text{AA}\text{-M}^+$  interaction is preferred while for  $\text{K}^+$ , with its more diffuse charge, addition of a hydrogen bond between the water and AA results in increased stabilization.

It should be noted that the differences in energy between many of the structures investigated are small. Relative energies are obtained from single-point calculations and do not include basis set superposition error. Even better calculations would be desirable to better distinguish between these different conformers. However, the consistency of the general structural conclusions, i.e., zwitterion vs non zwitterion, between theory and experiment does strengthen these conclusions.

Although the dissociation kinetics alone are an indirect probe of structure, structural information based on these kinetic experiments can be improved by carefully choosing model structures. Significant modeling has been performed to assess the quality of AlaOEt and Bet as models for VN and VZ, respectively. Calculations indicate that the AA, metal ion, and water interactions in the valine-containing compounds are well-mimicked by the model compounds for  $\text{M} = \text{Li}$  and Na clusters. For  $\text{M} = \text{K}$ , Bet is a good model for VZ, but AlaOEt is not a good model for VN. Modeling has also been performed to ensure that any differences in the radiative absorption and emission rates and any differences in transition-state entropies between these analogues do not effect our conclusions based on the experimental data. Numerical simulations of the dissociation experiment for the lithiated clusters show that radiative activation rates in the clusters are very similar. These simulations also reveal that while transition-state entropy effects the dissociation rate to some extent, the large differences measured in relative dissociation rates cannot be accounted for by differences in the radiative process, differences in transition-state entropy, or by the combination of these effects. Thus, these measurements should provide a good measure of the structure of these ions. This work also indicates that this experimental methodology can be extended to investigate the structure of clusters of  $\text{AA}\cdot\text{M}^+$  with multiple water molecules attached. The goal is to investigate the role of multiple water molecules on the structure of cationized valine and to determine how many

water molecules are required for valine to have the same structure in these cationized hydrated clusters as it does in bulk solution.

**Acknowledgment.** Financial support was generously provided by the National Science Foundation (Grant CHE-

0098109). This work was partially supported by the National Computational Science Alliance under Grant CHE010013N and utilized the NCSA SGI/CRAY Origin2000.

JA0106873